FULL RESEARCH ARTICLE

Effect of a process interruption on the mechanical properties of AlSi10Mg components produced by laser powder bed fusion (PBF-LB/M)

M. Moser[1,2] · S. Brenner[1,2] · L. Strauß[1,3] · G. Löwisch[1,3] · V. Nedeljkovic-Groha[1,2]

Abstract

Due to various causes, process interruptions during powder bed fusion of metal with laser beam (PBF-LB/M) can occur. This can be performed deliberately, e.g. as part of sensor integration or hybrid manufacturing. However, unplanned interruptions are also possible, for example, due to a power outage. In particular, long-term interruptions may result in significant quality losses, making it necessary to cancel the build job. Depending on the extent of the print job and the location of the interruption, this can mean a major economic loss. Most of the previous studies have found only minor reduction of the mechanical properties. However, these studies often dealt with the effect of planned interruptions and relatively short interruptions of about 1 h. Significantly longer interruption times are also realistic, especially when they occur overnight or during weekends. The aim of this study is to investigate the effects on the component quality of a process interruption when the manufacturing process is continued several hours after the interruption. For this purpose, the effects of different interruption durations (1, 4, 10 and 16 h) on the microstructure, hardness, tensile strength and fatigue properties of the PBF-LB/M-fabricated components made of AlSi10Mg were investigated. In addition, the layer shift resulting from the interruption is measured and described geometrically. The results show that for AlSi10Mg specimens in which the layer shift was removed and which are not highly loaded, an unplanned long-term process interruption up to 10 h does not result in a significant loss of quality under the considered conditions. Furthermore, it is apparent that the procedure for restarting the process is very important for the resulting component quality.

Keywords Powder bed fusion of metal with laser beam (PBF-LB/M) · AlSi10Mg · Process interruption · Additive manufacturing (AM) · Mechanical properties

1 Introduction

The significance of powder bed fusion of metal with laser beam (PBF-LB/M) is rapidly expanding in the industry. Reasons for this include a high degree of design freedom, enabling cost-effective production of highly complex and near-net-shaped structures even for small batch sizes. In addition, parts produced with PBF-LB/M nowadays partly exhibit better mechanical properties compared to cast components [1, 2].

As in all manufacturing processes, various anomalies and disturbances can occur in PBF-LB/M, which may have a negative impact on the robustness of the process as well as the component quality. The interruption of the manufacturing process represents such a realistic disturbance. It can be deliberately initiated, for example, in the context of the integration of smart components such as sensors or actuators as well as hybrid manufacturing [3–7]. However, a process interruption can also occur unplanned, e.g. as a result of a lack of powder or inert gas, a power outage or other unwanted occurrences during the process [8–11].

The potential consequences of an unplanned process interruption are various. First of all, there is an economic

✉ M. Moser
martin.moser@unibw.de

1 Department of Mechanical Engineering, University of the Bundeswehr Munich, Werner-Heisenberg-Weg 39, 85577 Neubiberg, Germany

2 Institute for Design and Production Engineering, Werner-Heisenberg-Weg 39, 85577 Neubiberg, Germany

3 Institute for Weapons Technology and Materials Science, Werner-Heisenberg-Weg 39, 85577 Neubiberg, Germany

(a)　　　　　(b)
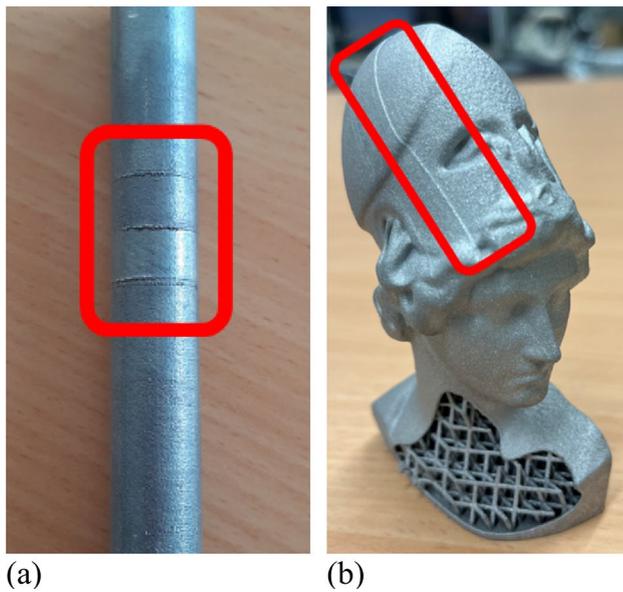
Fig. 1 Layer shift as a result of a process interruption. **a** Rod with multiple layer shifts caused by several process interruptions. **b** PBF-LB/M printed bust of Athena with layer shift due to a process interruption

loss due to the machine downtime. If the build job is cancelled, there is also a waste of materials such as powder or shielding gas. Due to the interruption and the associated cooling and shrinkage of the components, a circumferential mark is created when the process is continued, which is referred in VDI 3405 Part 2.8 as a layer shift [12] (Fig. 1). If they are not removed by machining, the marks cause not only a visual flaw but also a notch effect which has a negative impact on the mechanical properties of the component. Due to the interruption and the associated cooling of the parts, the powder bed and the entire system, there is also a risk of reduced bonding between the areas before and after the interruption when the build job is continued. In addition, the machine and generated components are slowly heated up by the PBF-LB/M process at the start of a regular build job and then remain at a stable temperature level until the build job is completed. However, if the build job is resumed after an interruption of several hours, the machine and the components undergo repeated heating and cooling phases, which could affect the quality of the components. If the build chamber is opened during the interruption or if the system is not completely sealed, oxidation, humidity or contamination of the powder bed can cause additional problems.

Depending on the size and quantity of the parts to be produced, a manufacturing process with PBF-LB/M can take several days, which is why the probability of such a disruption is much higher than with conventional processes. For this reason, the problem is particularly relevant for research institutions as well as for companies without 24/7

supervision, since the risk of an unnoticed long-term interruption over night or even over the weekend is especially high.

Several studies have already examined the effects of different interruption scenarios [3–11]. In all cases, the samples were printed regularly up to their test area where the process was paused deliberately. Depending on the investigated scenario, the duration (15 min to 24 h), as well as the state of the build chamber (open/closed) and the base plate heating (on/off) varied during the interruption. Mostly an aluminum alloy (AlSi10Mg, AlSi12) was processed [3, 5, 6, 8–10], but steel [4, 7], nickel alloys (Inconel 625, Inconel 718) [6] and Ti-6Al-4V [10, 11] were used as well.

The results of the studies are partly contradictory. While a few studies found a decrease in mechanical properties [3, 4, 11], most studies describe that there was no detectable influence of the interruption [5–7, 9, 10]. The opposite results can possibly be explained by the different interruption scenarios, materials, and interruption durations considered.

Some of the studies have also investigated the effects of a restart procedure. For example, in addition to multiple manual recoating to ensure a uniform powder bed, it has been tested whether multiple exposure are recommended instead of a regular single exposure [4, 5, 8]. This had the objective of developing a suitable procedure to minimize the risk of a negative influence of the process interruption. Following the restart procedure, the build job was finished in the regular manner. The results of Stoll et al. [4] and Richter et al. [8] indicated no significant impact of multiple exposure on the mechanical component properties, whereas Binder et al. [5] reported a decline in properties. This means that multiple exposure has no effect in the best case and negative effects in the worst case.

Most studies deal with relatively short interruption durations of 1 h or less, which is why the effects of long-term interruptions have not yet been adequately researched. In particular, the consequences for fatigue properties have not been clarified. This has only been considered for an interruption duration of 1 h by Richter et al. [8]. In addition, the resulting layer shifts have been mentioned, but their geometry and dimensions have not yet been described in the literature.

An interruption often results in anomalies of the temperature history of the parts to be manufactured, which is why long-term interruptions in particular have the potential to influence the properties of the parts [12]. Hence, the aim of this study is to generate further knowledge regarding the consequences of long-term interruptions on the mechanical properties. The effects of different interruption times on porosity, microstructure, hardness and tensile properties are investigated. In addition, fatigue tests for an interruption duration of 10 h were carried out and the layer shift was geometrically described. Based on the findings, the waste

Table 1 Default process parameters for specimen fabrication

Parameter set	Laser power (W)	Scan speed (mm/s)	Hatch distance (mm)	Slice thickness (mm)	Base plate temperature (°C)	Scan strategy (−)	Rotational angle (°)
Hatch	350	1650	0.13	0.03	150	Stripes	67
Contour	300	730	/				

rate of PBF-LB/M could be reduced and thus the economic efficiency of the process could be increased.

2 Materials and methods

For this study, all samples were produced on a standard SLM125HL® from SLM Solutions with the parameter set listed in Table 1. Every build job started after the required build plate temperature of 150 °C and an oxygen level in the build chamber of 0.05% were reached. The argon shielding gas flow was set to 4 m/s. The gas atomized AlSi10Mg powder with a particle size distribution of 20–63 μm was purchased from the machine manufacturer SLM Solutions and used in recycled condition in this study.

In the context of this study, the scenario of a process interruption due to a power outage was investigated. This involved simulating conditions as if there were a real power outage, with the build chamber remaining sealed and both the base plate heating and shielding gas flow deactivated. The study considered four different interruption durations: 1, 4, 10, and 16 h. To assess the impact of the process interruption on component quality, the layout shown in Fig. 2a was printed once for each interruption duration. Every build job consisted of five notched cubes, six smaller and 12 larger cylinders. The different sample heights were adjusted by using support structures to ensure that the interruption level was positioned within the testing area of all specimens (Fig. 2b). Up to a height of 55.5 mm, the specimens were printed regularly. After exposing the powder layer, the build job was paused deliberately and the base plate heating and gas flow were deactivated.

The notched cubic samples with dimensions $8 \times 10 \times 6$ mm^3 served three main purposes—examining the geometry of the layer shift and investigating the microstructure and hardness following DIN EN ISO 6507-1 [13] and VDI 3405 Part 2 [14]. The notch on these samples marked the interruption level, facilitating its identification in cross-sections. A Keyence VR-5200® 3D profilometer was used to measure the geometry of the layer shift. To prepare metallographic sections for hardness and microstructure analyses, the samples were ground and polished along the plane shown in Fig. 2c. Microstructure examination required additional etching of the samples with 5% sodium hydroxide

solution. Microscopic analysis was carried out using a digital microscope Keyence VHX-3000® and a Zeiss Ultra 55® SEM. For HV 0.1 hardness testing, a QATM QNESS 60 A + EVO® was used, producing the test pattern as shown in Fig. 2d. The red dashed line marks the interruption level on which one measurement was performed. Additionally, four more measurement points were placed above and below this plane, spaced at intervals of 0.5 mm.

The small grey cylinders depicted in Fig. 2a and b are tensile test specimens according to DIN 50125-B5×25 [15]. These specimens were initially produced as plain cylinders with a diameter of $\varnothing 10 \times 72$ mm^3 and later machined by turning. Tensile tests were performed according to DIN EN ISO 6892-1 [16] using a ZwickRoell Z100/SN3A® machine. A Keyence VHX 3000® digital microscope and a Zeiss Ultra 55® SEM were used for fracture surface analysis.

For assessing fatigue resistance, specimens following DIN 50113 [17] ($\varnothing 15 \times 72$ mm^3 and $\varnothing 15 \times 120$ mm^3) were manufactured, as shown in the larger cylinders in Fig. 2a and b. There are two types of fatigue specimens—"as-built" specimens, which were 3D printed in their final shape, and "machined" specimens, initially shaped as $\varnothing 15 \times 120$ mm^3 cylinders and then post-processed by turning. To evaluate time-dependent strength, the pearl string method following DIN 50100 [18] was used with $R = -1$, employing a SincoTec POWER ROTABEND® rotary bending test machine. Each stress level was tested at least twice. During the study, it became evident that the number of 12 fatigue specimens was insufficient for generating statistically significant results. Consequently, fatigue specimens were manufactured separately with a 10-h interruption, with each variant comprising 30 specimens. To avoid potential variations in temperature history affecting the specimens, the large cylinders, intended as fatigue specimens, were still printed within the layout shown in Fig. 2a. They were used for measuring the interruption marks and additional hardness tests. Five samples per interruption period were selected to measure the marks. For the hardness measurements, three samples with ten- and 16-h interruptions and the same number of reference samples were used. Like the cubic samples, these were first embedded and prepared by grinding and polishing. The hardness measurements were carried out on the same device and with the same settings as for the cubic specimens, but
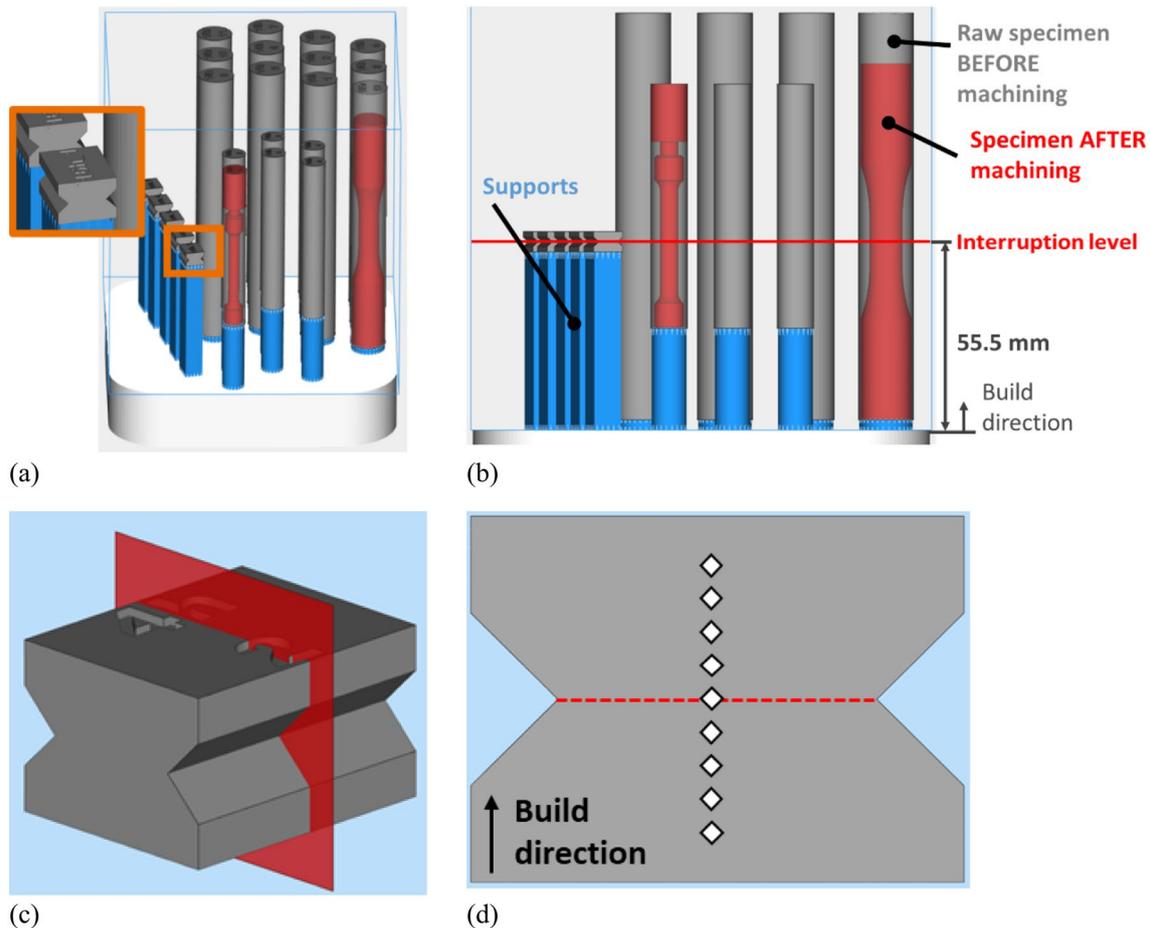
Fig. 2 Build layout with notched cubes, tensile and fatigue specimens (**a**), marking of the interruption level (**b**), ground plane of cubic specimens (**c**) and test pattern for HV 0.1 hardness test (**d**)

in a range of ± 15 mm below to above the interruption level instead of ± 2 mm for the cubes.

Following the specified interruption duration, a restart procedure was performed. This involved inerting the build chamber and switching on the base plate heater as well as the shielding gas flow. According to the temperature sensor integrated in the machine's platform below the base plate, the desired temperature of 150 °C was reached after approximately 3 min. It was assumed that the base plate, machine components, and the powder bed had not yet attained the desired temperature. Consequently, a total waiting time of 15 min was observed before conducting multiple manual recoating operations to ensure the uniformity of the powder layer on all samples. Based on the findings of Stoll et al. [4], Binder et al. [5] and Richter et al. [8], no multiple exposure was carried out and the build job was therefore restarted using the default process parameters listed in Table 1 on the new recoated powder layer.

3 Results and discussion

3.1 Results during the build job

After the interruption and a 15-min preheating time, a manual recoating was carried out. It was observed that especially after longer breaks exceeding 10 h, a single recoating process is not sufficient to achieve a homogeneous powder layer on all samples. Figure 3a shows an image of the machine's internal layer control system (LCS). This system captures camera images of the powder bed and checks it for anomalies, which are highlighted in color. As can be seen, powder was only deposited in the lower area of the build plate, which means that the amount of applied powder in a regular recoating process is not sufficient to create a homogeneous powder bed across all components. This indicates that the samples and the powder bed are not entirely heated up to the temperature before the interruption, which means a smaller thermal expansion in build direction and therefore a gap between the last solidified layer before the interruption and

(a)

(b)
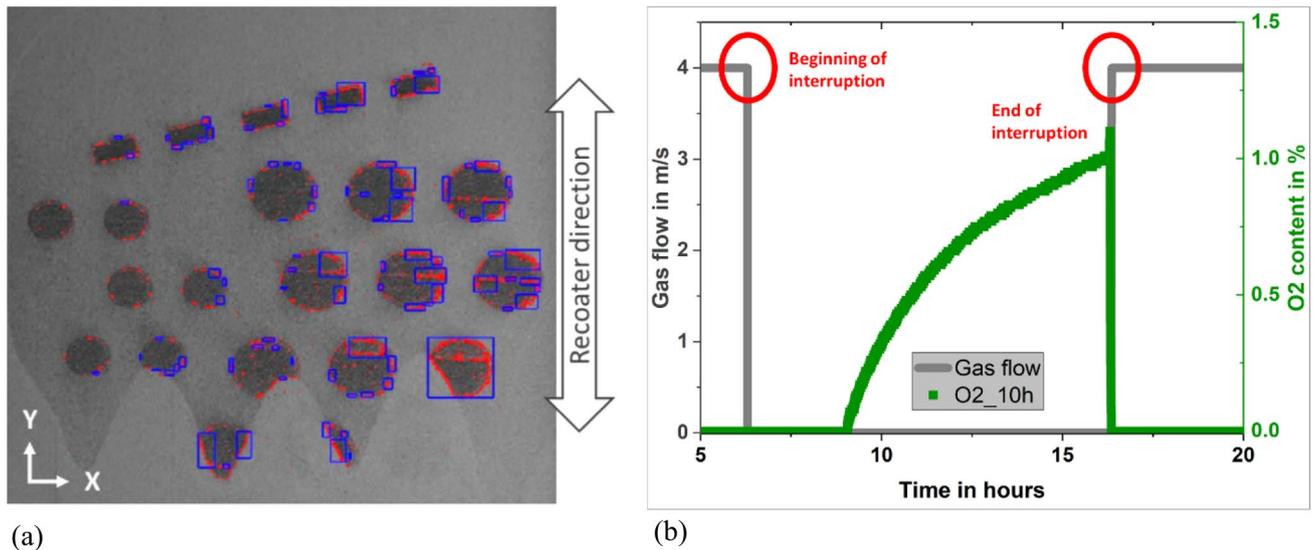
Fig. 3 **a** Image of the layer control system (LCS) installed in the SLM125® shows an inhomogeneous powder bed due to insufficient powder quantity during the recoating process. **b** Shielding gas flow velocity and oxygen content in the building chamber during a 10 h interruption

the recoating level. To fill this gap, a considerably greater quantity of powder is required than in a regular recoating process. Hence, a multiple manual recoating as well as a significantly longer heating time before restarting the build job are necessary to heat the components and powder bed to the desired temperature as well as achieving a homogeneous powder bed. This is recommended to minimize the risk of a negative impact due to a process interruption.

In addition to the described cooling of the machine during the interruption, it must be expected that the machine is not completely sealed. For this reason, there is a risk of an increase in the oxygen content in the build chamber during the interruption. Figure 3b shows the flow velocity of the shielding gas and the oxygen content at the ceiling of the build chamber during a production interruption of 10 h. The drop and the rise in the flow velocity mark the beginning and the end of the interruption. At the beginning of the interruption, the oxygen level initially remains constant at 0%. After a standstill period of approximately 2.7 h, the oxygen content slowly rises to a maximum value of 1%. By flooding with argon again and switching on the inert gas flow during the restart procedure, the oxygen content increases briefly to 1.1% and then drops to 0% again before the build job is resumed and remains at this level until the end of the build job. This curve indicates that the oxygen content continues to increase with longer interruption duration, which is not the case. A maximum oxygen content of 1.1% was also recorded for a 16-h interruption. In contrast, the oxygen content remains at 0% during an interruption of 1 h and rises to a maximum value of 0.6% after 4 h. This shows that the SLM125® is not completely leakproof. Possible explanations are not completely sealed system boundaries such as

the build chamber door or the pipework as well as the elimination of the overpressure when the gas pump is switched off. However, in the study conducted by Stokes et al. [9], the samples and powder were exposed to the atmosphere for up to 24 h with no significant effect. For this reason, the relatively small increase in oxygen in this study is not considered to be significant.

3.2 Layer shift

As expected, the specimens also show the previously mentioned layer shift (Fig. 4a). If these marks are not removed by subsequent machining, they represent a visual flaw and result in a notch effect. Just by visual inspection of the cylindrical specimens, it is noticeable that the layer shift is not a uniform circumferential defect. Instead, it is an offset of the upper half of the specimens printed after the interruption (Fig. 4b). Figure 4c shows the size of the interruption marks at different interruption durations for the cubic and fatigue specimens. It can be seen that the marks have approximately the same size for both geometries. Furthermore, a clear trend can be seen up to an interruption duration of 10 h. The mean size of the marks is 0.03 mm for 1-h samples and 0.06 mm for 4-h samples. With an average of 0.1 mm and a maximum of 0.12 mm, the largest marks occurred at samples with a 10-h interruption, followed by an average size of almost 0.08 mm at 16 h. In addition, on all examined fatigue specimens it was observed that this does not appear to be a permanent shift. About 8 mm after continuing the build job, the two halves of the specimen converge again and the offset disappears (Fig. 4d). Since the cubic specimens were too small and the tensile specimens were not examined

(a)   (b)   (c)   (d)
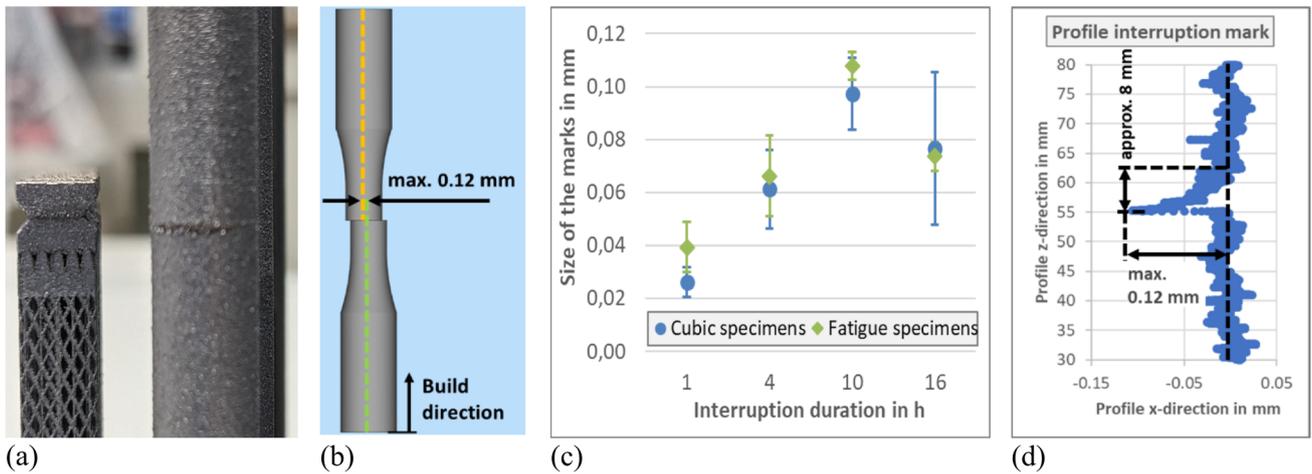
Fig. 4 Geometry of the layer shift. Layer shift on the real specimens (**a**), shift on the example fatigue specimen (**b**), size of the interruption marks depending on the interruption duration for cubic and fatigue specimens (**c**) and profile of the layer shift on the example fatigue specimens (**d**)

(a)   (b)
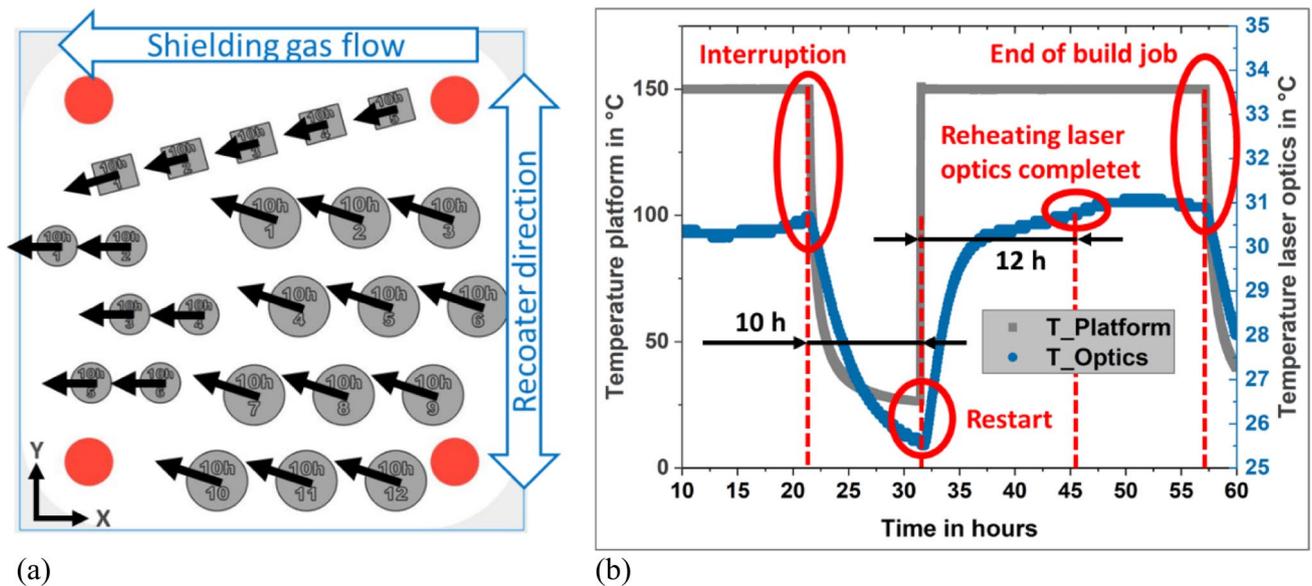
Fig. 5 Offset direction of the layer shift (**a**) and temperature history of the platform and the laser optics (**b**)

in this respect, no statement can currently be made about this behavior for other geometries.

A more precise analysis of the layer shift reveals that there is a preferred orientation in negative x-direction (Fig. 5a). This phenomenon has occurred in all build jobs performed in this study, which strongly indicates a systematic effect.

A first possible explanation is the shielding gas flow, whose direction coincides with the preferred offset direction. Although this is considered a less likely cause due to the low flow velocity of 4 m/s, it cannot be ruled out as a cause at the moment.

Another possible explanation might be material shrinkage due to cooling during machine downtime, not only of the samples and the powder bed, but also of the base plate as described by Binder et al. [5]. It is conceivable that the screw connection of the base plate loosens due to cooling, which could result in a change of the specimen position in the build space. However, this alone is unlikely to be the sole cause of the preferred direction, since in this case a randomly varying offset direction would have to be expected. Even if the temperature is not uniform throughout the build space, leading to different dimensions of the layer shift depending on the

position of the specimen, there should be no clear preferred direction. Despite their different sizes, both the cubic and the fatigue specimens have almost the same offset, which also argues against thermal shrinkage as the main cause.

The currently most plausible explanation for the preferred offset direction is a thermal contraction of the entire system, including the laser optics. This effect could be further enhanced by a temperature-induced change in the refractive index in the laser optics. This phenomenon, known as thermal lensing, causes a shift in the focus plane and the spot diameter [19, 20]. In highly precise systems such as laser optics, even supposedly small temperature differences of a few degrees can have significant effects on the positioning accuracy of the laser spot. The distance between base plate and laser entry window of the SLM125® is about 340 mm. For an offset of 0.12 mm, this corresponds to a minor angular error in laser positioning of 0.02°.

Figure 5b compares the temperature curves recorded by sensors in the platform below the base plate and the optical bench of the machine. As can be seen, the platform and laser optics cool down from their operating temperature (platform = 150 °C; laser optics = 30.7 °C) to a temperature of about 26 °C within the interruption period of 10 h shown here. After the end of the interruption period, a restart procedure was carried out in which the base plate heating and the shielding gas flow were switched on again. While the platform reached the set temperature of 150 °C after about 3 min, the laser optics needed up to 12 h to achieve the same temperature as before the interruption. In addition, this behavior matches the results of the 3D scans on the fatigue samples in Fig. 4d, which show that the offset of the layer shift is not permanent, but is eliminated after about 8 mm. This will probably only happen when the temperature of the laser optics approaches the value before the interruption again and reaches a certain value. This temperature can be determined by calculating the production time until the misalignment disappears. With a layer thickness of 30 μm, 8 mm equals a number of 267 layers. An average layer duration of 31.8 s results in a production time of 2.36 h after continuing the build job until the mark has disappeared. At this time, the optical bench reaches a temperature of 28.3 °C, reducing the temperature difference from initially 4.7 °C to about 2.4 °C compared to the temperature before the interruption occurred. The temperature of the laser optics rises rapidly at first and then becomes flatter. This could explain why the offset is already compensated after about 2.36 h of runtime, instead of the expected 12 h. This also indicates that there is a positioning error in the first few layers at the start of every build job when the laser optics is still cold. These first layers usually consist of supports or are removed when the samples get cut from the build plate. Unfortunately, preheating the laser optics of a commercially available SLM125® is not
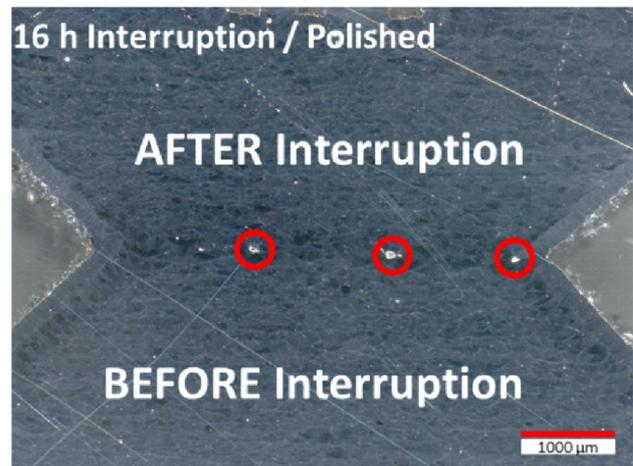
Fig. 6 Microscope images for analysis of porosity at a polished sample with a 16-h interruption

possible because the machine is not equipped with a heating system to control the temperature of the optical bench.

The correlation between the size of the interruption marks and the interruption duration shown in Fig. 4c might also be caused by a positioning error due to the cooling of the machine, the laser optics, the components and the powder bed. As the duration of the interruption increases, these cool down more, which increases the temperature difference compared to before the interruption. The smaller the temperature difference when the build job is continued, the smaller the positioning error might be. It is not yet clear why the marks of the 16-h samples are smaller than those of the 10-h samples. However, it is assumed that the reason for this can also be found in different temperature profiles. In addition, a combination of several effects mentioned in this study, such as thermal lensing, contraction of the laser optics and an increased first powder layer thickness when continuing the build job, is conceivable.

3.3 Porosity and microstructure

The results of the porosity investigations show that a distinct increase in porosity can only be recognized for the 16 h samples (Fig. 6). There is no significant change in porosity for all other investigated interruption times.

The first finding in the microstructure is a dark area in the interruption zone (red box in Fig. 7). This anomaly has also been observed in previous studies [5, 9, 10]. Binder et al. [5] opened the chamber during the interruption, which is why they may have suspected increased oxidation. According to Mahtabi et al. [10], who observed the dark area with open and closed build chamber, the changed temperature history due to the interruption could be responsible for this discoloration.
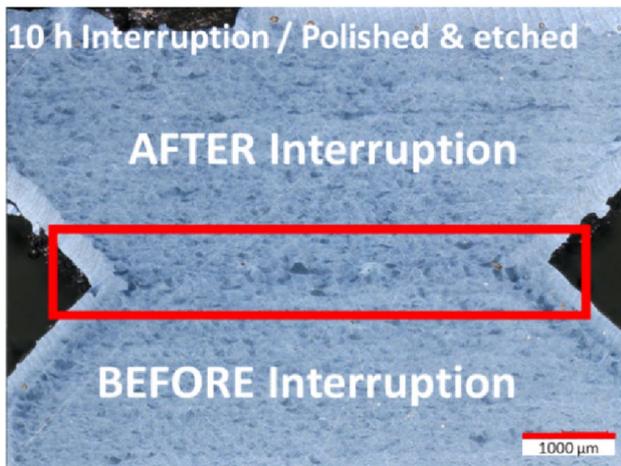
Fig. 7 Microscope images for analysis of microstructure of a polished and etched sample with a 10-h interruption

Figure 8 shows representative SEM images of the areas 2 mm below (a), in (b) and 2 mm above (c) the interruption of a 10 h-sample. It can be seen that the Al cells below and above the interruption have an elongated orientation in the build-up direction and are surrounded by a Si eutectic, also shown in the literature [6, 8, 9]. The grains preferably grow in the direction of the heat flow—in this case in the negative z-direction. Unlike in the areas before and after the interruption, the microstructure in the interruption area appears to have slightly more of the fine and round grain structures. This could indicate an interrupted or altered heat flow due to the process interruption and could also be a possible explanation for the discoloration in the interruption plane. However, this change is only a minor and localized effect. As already reported in several studies, no clear changes in the microstructure due to the interruption have been found within these investigations either [3, 6, 10, 11]. For this reason, the studies were limited to the reference and 10 h samples. The broken Si boundaries shown by Stokes et al. [9] and in Fig. 8a also occurred in the reference samples,

whereas the shift in the microstructure mentioned by Richter et al. [8] could not be detected.

3.4 Hardness

Figure 9a shows the hardness values of the cubic samples at different z-positions relative to the interruption level for the investigated interruption times. The two horizontal black lines represent the range of variation based on the mean value and the standard deviation of the reference samples (128 ± 4 HV 0.1) and visualize the variance of the measurement results. The mean values and deviation ranges of all interruption times are shown in Table 2. For all interruption times, slightly increasing hardness values with increasing z-position can be recognized in the area below the interruption, which remain at a constant hardness level in the area after the interruption. For the 4 h and 16 h samples, the highest hardness values (136 ± 1 HV0.1 and 135 ± 8 HV0.1) were found at the interruption level. The reference samples show a similar trend of increasing and then constant values. In order to verify this trend over a greater build height, some of the fatigue samples shown in Fig. 2a and b, were used for this purpose. Figure 9b shows the hardness curves of the fatigue specimens for the investigated interruption durations. Compared to the cubic specimens, the hardness of the fatigue specimens is higher, as a different temperature history is present. Considering the small scatter band of the mean values and the relatively large standard deviations, no trends can be recognized depending on the z-position. As already observed for the cubic samples, the 16 h fatigue samples also show that the hardness values in the interruption level are slightly higher than in the rest of the sample. This could be due to the slightly finer grain structure shown in Fig. 8b. However, considering the large scatter of the values and the fact that almost all values are within the scatter band of the reference samples, the increased hardness values in the interruption zone might also be a coincidence.

A possible explanation for the lower hardness of the cubic samples in the area before the interruption might be poorer
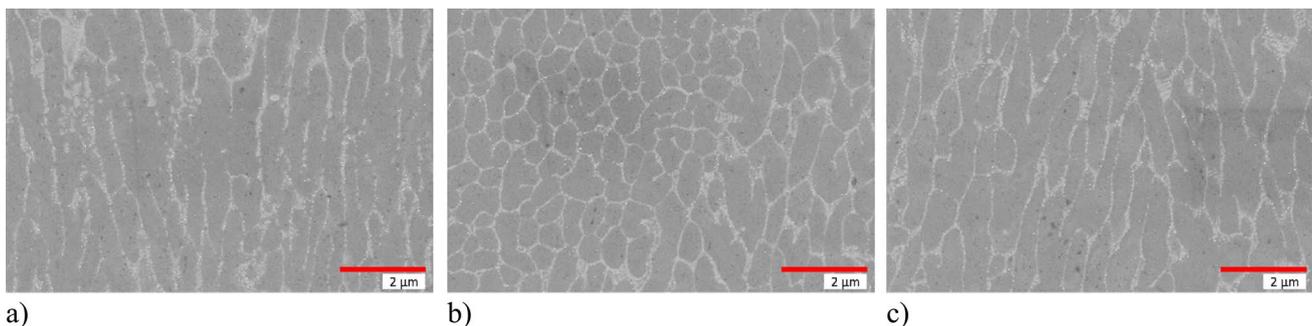
Fig. 8 SEM images 2 mm below (**a**), in (**b**) and 2 mm above (**c**) the interruption of a 10 h-sample

(a)   (b)
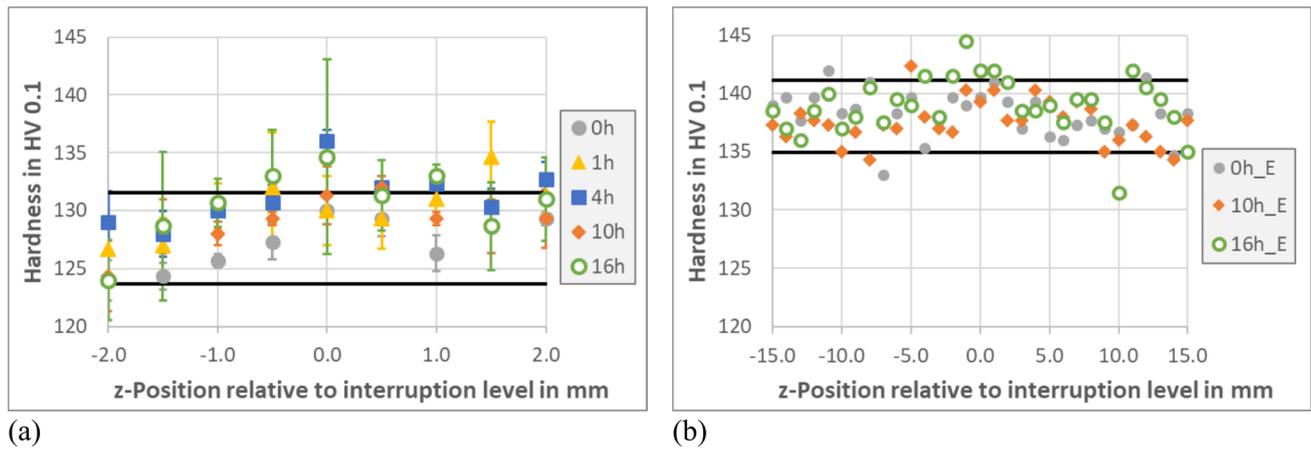
Fig. 9 Hardness profile of the cubic specimens (**a**) and the fatigue specimens (**b**) at different positions relative to the interruption level and interruption durations. The black horizontal lines represent the range of variation of the reference samples

Table 2 Mean values and standard deviation of the hardness and tensile tests (values in brackets include all six tensile specimens)

Interruption duration (h)	Hardness values cubic samples (HV 0.1)	UTS (MPa)	ε_f (%)	YS (MPa)
0	128 ± 3.8	460 ± 6.3 (466 ± 7.7)	3.9 ± 0.3 (4.4 ± 0.6)	281 ± 1.8 (282 ± 1.7)
1	129 ± 3.7	474 ± 2.4 (475 ± 2.0)	4.7 ± 0.2 (4.8 ± 0.2)	280 ± 1.4 (281 ± 1.4)
4	131 ± 2.9	469 ± 10.7	4.3 ± 0.7	285 ± 1.2
10	128 ± 4.0	478 ± 4.7	5.0 ± 0.6	285 ± 1.7
16	129 ± 5.3	457 ± 17.8	$3,6 \pm 0.5$	285 ± 6.7
VDI 3405 Part 2.1 [1]	112…124	353…482	2…5	210…272
p-value	0.16	0.015	0.001	0.132

heat flow due to the perforated block supports directly below the samples. The area below the interruption level may not be sufficient to ensure uniform heat dissipation, possibly leading to heat accumulation in the lower sample area, which might influence the properties of the samples. This assumption fits with the higher hardness level of the fatigue specimens. These were printed on solid volume support and are significantly larger than the cubic samples, which favors the heat flow. Furthermore, the examined area is notably farther from the support structures, indicating that consistent heat dissipation may have already occurred in this region. This shows that the cubic samples are probably too small and therefore unsuitable for valid measurements of hardness profiles over the build height.

In addition to the qualitative evaluation of the changes, an analysis of variance (ANOVA) with an α-level of 5% was performed to assess the significance of the changes at different interruption durations. The *p*-value serves as the evaluation parameter. This evaluates whether there is a significant difference between the values of the groups in relation to their respective variance. A *p*-value smaller than 0.05

indicates a significant difference between the groups and thus an influence of the variable, in this case the interruption duration. The ANOVA shows a minimum *p*-value of 0.16, which confirms the findings described above that there is no significant change in hardness due to an interruption.

The results agree with the findings of the microstructural tests, where only minor changes were detected. This is consistent with the results of Terrazas et al. [6], Mahtabi et al. [10] and Stokes et al. [9] who found no significant changes in hardness values. However, under the same conditions, they only considered interruption durations of 1–12 h.

3.5 Tensile tests

The results of the tensile tests are also shown in Table 2 as well as Fig. 10. Again, an ANOVA was performed to provide a quantitative indication about the significance of the differences due to the interruption duration. The ultimate tensile strength (UTS) varies between 460 and 478 MPa depending on the duration of the interruption. A *p*-value of 0.015 indicates a significant influence of the interruption duration.

(a) (b)
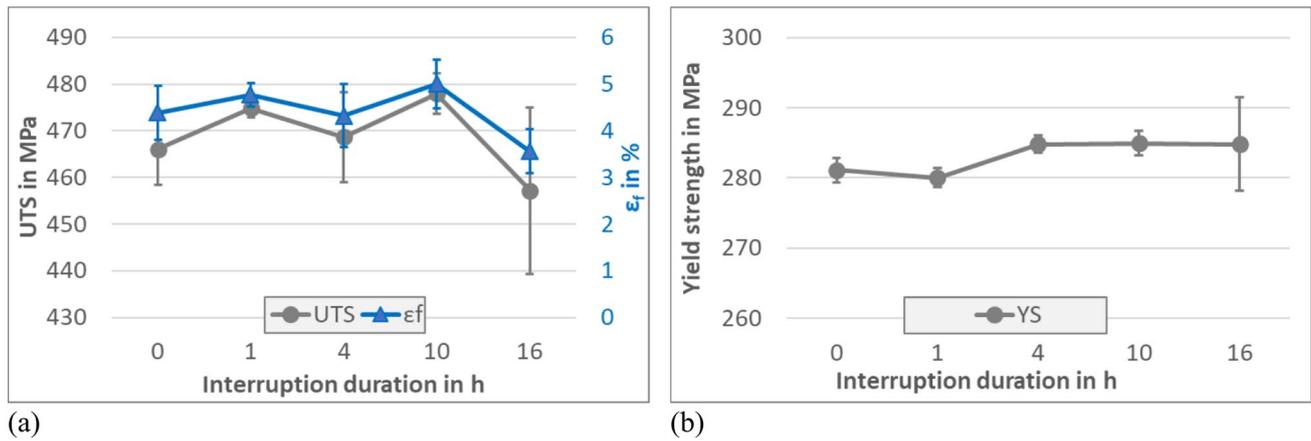
Fig. 10 Results of tensile tests: **a** elongation at break and ultimate tensile strength; **b** yield strength

The elongation at break (ε_f) is also significantly influenced by the duration of the interruption (p-value $=0.001$). It varies between 3.6% and 5.0%. The yield strength (YS), on the other hand, is not affected (p-value $=0.132$) and varies in the range from 280 to 285 MPa (Table 2). Compared to the data given in the material data sheet for AlSi10Mg in VDI 3405 Part 2.1 [1], the tensile strength values determined generally achieve very good results.

(a) (b)

(c) (d)
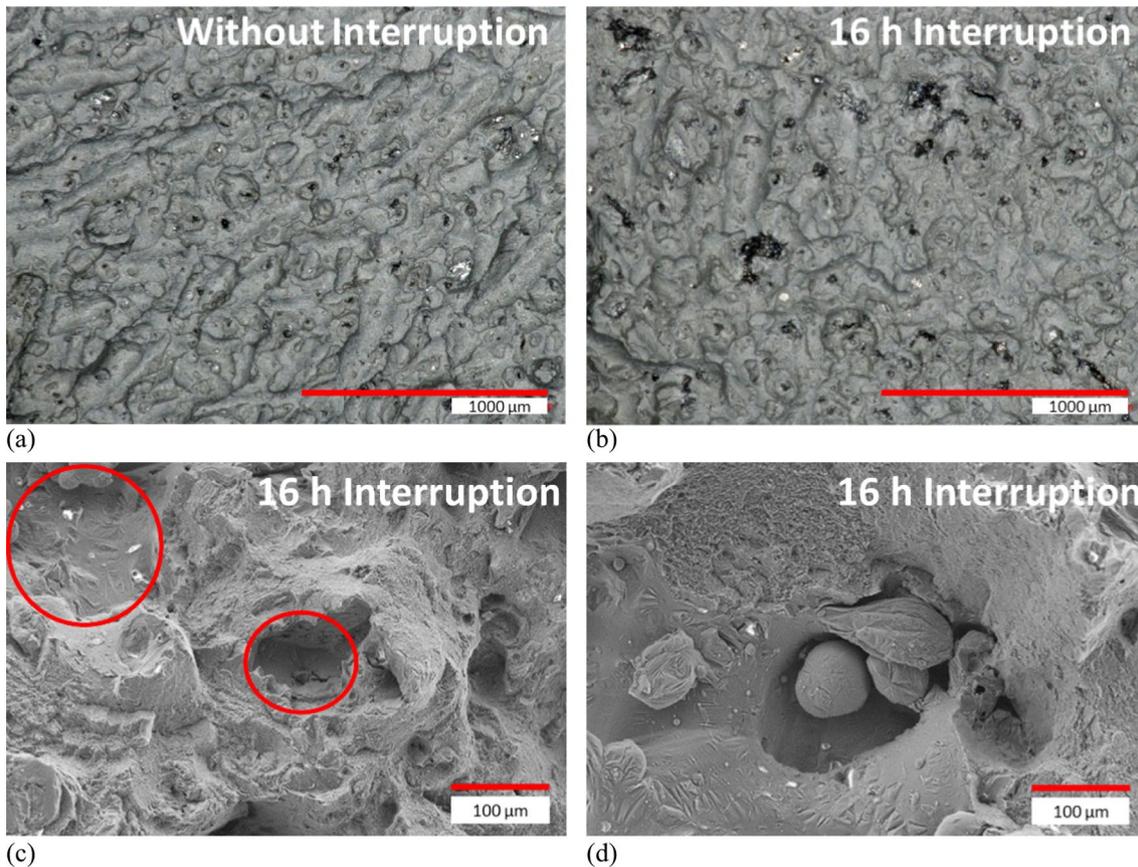
Fig. 11 Results of fracture surface analysis: **a** Digital microscope image of a fracture surface from a reference sample with less and small defects; **b** Digital microscope image of a fracture surface from a 16-h sample with many LoF defects; **c** SEM images of flat surfaces; **d** SEM images of unmolten powder particles

Looking at Fig. 10a, it is noticeable that UTS and ε_f show an almost parallel zig-zag pattern of increasing and decreasing values. This suggests a correlation between the two values, but this has not been mentioned in other studies. The yield strength, on the other hand, is not affected by an interruption lasting up to 10 h (Fig. 10b). In case of an interruption period of 16 h, there is a significant increase in the variation of tensile strength as well as yield strength. This indicates that the probability of critical defects such as lack of fusion (LoF) is significantly increased in case of a 16-h interruption, thereby reducing the robustness of the PBF-LB/M process. For unknown reasons, half of the reference specimens (0) as well as the 1-h specimens failed in the upper region outside the strain gauge extensometers. Even if the samples are broken in the cylindrical area of the specimens and the values can therefore be utilized, only the three samples that broke within the area of the extensometer were considered for the evaluation of the 0 h and 1 h interruptions. In Table 2, the values of all six samples are added in brackets.

Up to an interruption duration of 10 h, the results confirm the findings from the microstructure analysis and the hardness measurement, in which only minor changes were detected. The worse properties at a 16-h interruption might be caused by an increase of defects in the interruption zone. This is shown by a simultaneous decrease in tensile strength and elongation at break as well as an increase in the variance. Up to an interruption duration of 10 h, the results of this study are consistent with the findings of most studies, which state that the tensile strength properties are not significantly affected by a machine breakdown. However, the studies only tested a maximum duration of 12 h under the same conditions, so any differences could be due to the longer interruption period.

3.6 Fracture analysis

As mentioned above, half of the reference samples without interruption as well as the 1-h-specimens broke in the upper region outside the strain gauge extensometers. This confirms the finding that an interruption duration of 1 h has no significant effect on the mechanical properties. Under the mentioned restrictions, it can be seen that with increasing downtime, more specimens tend to fail in the area of the interruption zone.

Figure 11 shows examples of the fracture surfaces from a reference specimen (a) and a 16-h specimen (b). The digital microscope images show that with increasing interruption time, the proportion of defects that appear darker on the fracture surfaces increases. Figure 11c and d show SEM images of these defects. Flat surfaces (c) and unmolten powder particles (d) are a clear indication for lack of fusion (LoF). This supports the findings from the tensile tests that an interruption time of 16 h can have a negative effect on the mechanical properties.

3.7 Fatigue tests

In the context of this study, a distinction is made between two machining states of the fatigue specimens. These are as-built as well as machined specimens, which were produced without an interruption or with an interruption duration of 10 h. Three of the four types are shown in Fig. 12, while machined samples with and without interruption do not differ visually.

Figure 13 shows the fatigue life diagram in which the stress amplitude is plotted over the number of cycles to failure in a double logarithmic manner. Furthermore, the values for the mean roughness depth Rz as well as the theoretically endurable stress amplitude for 200 k cycles are shown. Comparing the properties of machined specimens without interruption (grey) with those of as-built specimens without interruption (blue), it can be seen that the as-built specimens fail significantly earlier (Fig. 13a). This can be explained by the higher roughness of the as-built specimens (Rz = 21.45 μm). The fatigue properties are mainly determined by surface near inhomogeneities and notches such as pores and the surface roughness [21–25]. This is also shown when comparing the as-built specimens
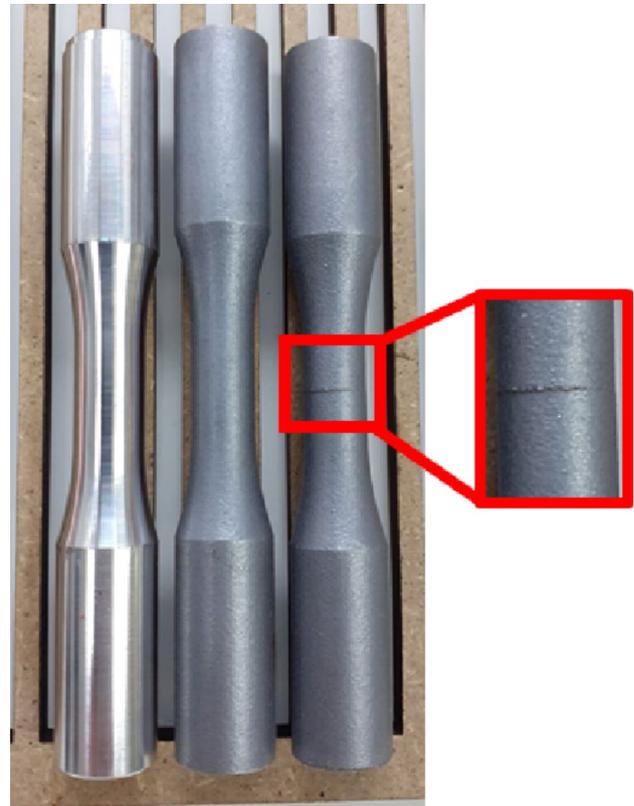
Fig. 12 Types of fatigue specimens: machined fatigue specimens (left), as-built specimens without interruption (center) and as-built specimens with a 10 h interruption (right)

Sample type	Rz (μm)	$\sigma_{a,200k}$ (MPa)
NO interruption machined	9.00±1.90	128.2
NO interruption as-built	21.45±3.74	83.8
WITH interruption as-built		61.1

(a)

Sample type	Rz (μm)	$\sigma_{a,200k}$ (MPa)
NO interruption machined	9.00±1.90	128.2
WITH interruption machined		127.5

(b)
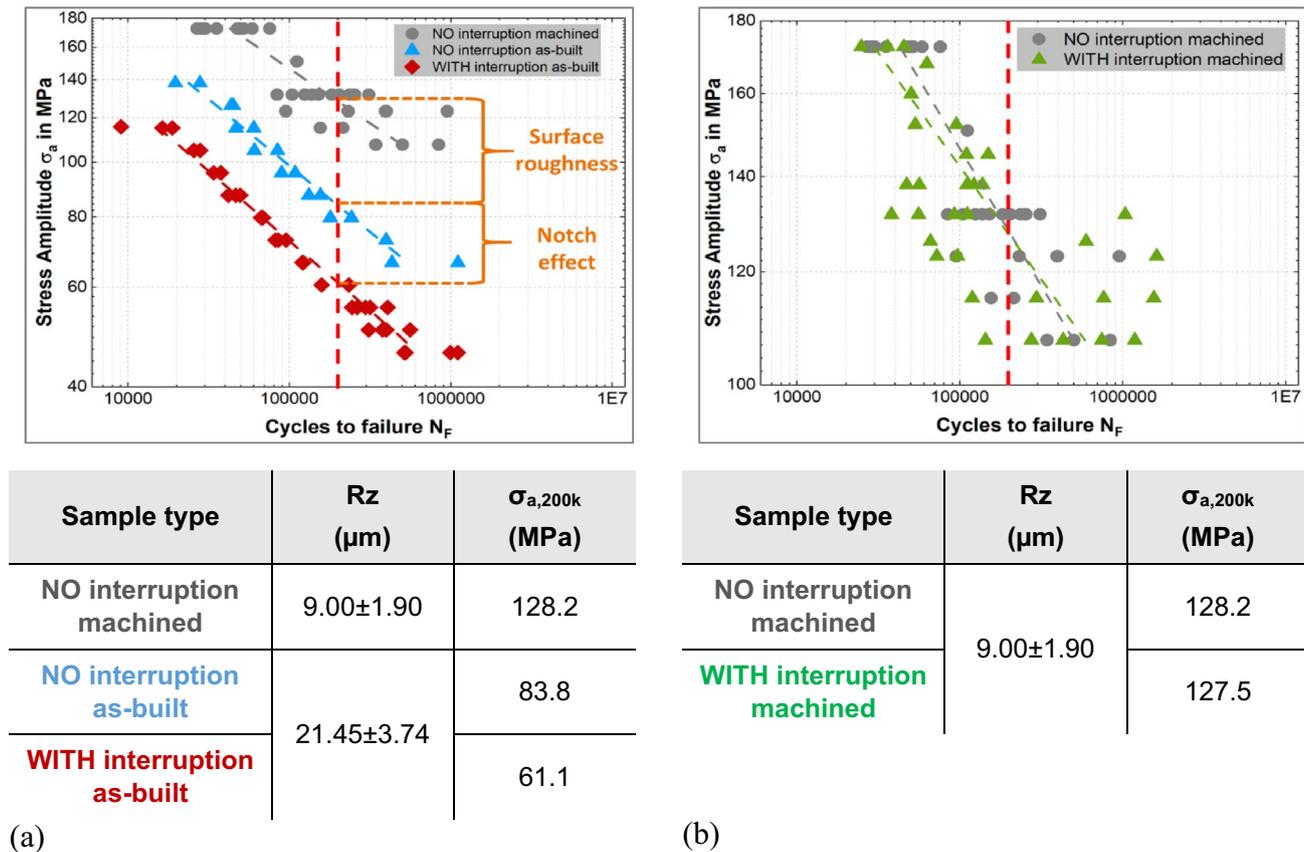
Fig. 13 Fatigue life diagram: **a** Comparison of as-built specimens without (blue) and with a 10-h interruption (red) with machined specimens without interruption (grey). **b** Machined specimens without (grey) and machined specimens with a 10-h interruption (green)

without interruption with those with interruption (red). The lower number of cycles to failure can be explained by the notch effect of the layer shift. The layer shift represents a single notch with a depth up to 0.12 mm and is thus about six times higher than the Rz. More surprising are the results of the machined specimens (Fig. 13b). Here, no significant difference can be seen between the specimens without (grey) and with interruption (green). It merely appears that the variance of the samples with interruptions is slightly higher. The results confirm the conclusions of Richter et al. (2021) [8] that the fatigue strength of machined specimens is not affected by a process interruption.

4 Conclusions

In this study, the effects of an unplanned process interruption on the properties of PBF-LB/M samples made of AlSi10Mg were investigated. A power outage scenario with four different interruption durations of 1, 4, 10 and 16 h was considered. Before continuing the build job, a

multiple manual recoating was required to achieve a uniform layer of powder on all samples. As expected, the specimens printed in this study formed the layer shift known from other studies. However, this is not a uniform circumferential mark, but rather a lateral offset of the sample area which was produced after the interruption. Up to a duration of 10 h, the size of the marks correlates with the interruption duration. Furthermore, the offset appears to be not permanent and unrelated to the specimen geometry, as it shows approximately the same size for cubic and fatigue specimens. In addition, a preferred direction of this upper area offset was observed in all build jobs, which is an indication for a systematic effect. The most conclusive explanation so far can be found in a thermal contraction of the laser optics due to the cooling during the machine downtime.

While no change in the microstructure could be observed, a clear influence of the interruption on porosity and mechanical properties was only detectable for durations of 16 h. For this, a decrease in tensile properties and increased variance were observed, probably caused by more defects in the interruption level. The fracture location is also affected by the

interruption, as increasing interruption duration also resulted in more specimens breaking in the interruption level. The fatigue properties of the as-built specimens were reduced by the notch effect of the interruption mark. In contrast, the comparison between machined specimens, where the mark was removed by turning, shows no clear difference.

In conclusion, for AlSi10Mg samples where the interruption mark has been removed and which are not highly loaded, an unplanned process interruption up to a duration of 10 h does not result in a significant loss of quality under the considered conditions. Even if the overall quality losses due to an interruption are not significant, a suitable restart procedure should be defined and performed to minimize the risk of negative effects. In addition to investigating the effects on component properties, especially for as-built parts, it is also important to examine how affected components can be handled. There is also further research potential in understanding the formation, orientation and characteristics of the interruption marks.

Declarations

Conflict of interest For this research, there is no conflict of interest for all authors.

References

1. VDI Verein Deutscher Ingenieure e.V. 2020–08–00, Additive Fertigungsverfahren—Pulverbettbasiertes Schmelzen von Metall mittels Laserstrahl (PBF-LB/M): Materialkenndatenblatt Aluminiumlegierung AlSi10Mg, Vol. 25.020
2. Kempen K, Thijs L, van Humbeeck J, Kruth J-P (2012) Mechanical properties of AlSi10Mg produced by selective laser melting. Phys Procedia 39:439–446. https://doi.org/10.1016/j.phpro.2012.10.059
3. Hammond V, Schuch M, Bleckmann M (2019) The influence of a process interruption on tensile properties of AlSi10Mg samples produced by selective laser melting. Rapid Prototyping J 25:1442–1452. https://doi.org/10.1108/RPJ-04-2018-0105
4. Stoll P, Spierings A, Wegener K (2019) Impact of a process interruption on tensile properties of SS 316L parts and hybrid parts produced with selective laser melting. Int J Adv Manuf Technol 103:367–376. https://doi.org/10.1007/s00170-019-03560-1
5. Binder M, Leong C, Anstaett C, Schlick G, Seidel C, Reinhart G (2020) Effects of process interruptions on the microstructure and tensile properties of AlSi10Mg parts manufactured by laser-based powder bed fusion. Procedia CIRP 94:182–187. https://doi.org/10.1016/j.procir.2020.09.035
6. Terrazas CA, Mayoral FL, Garcia OF, Hossain MS, Espalin D, Fernandez A, Murr LE, Wicker RB (2021) Effects of process interruptions on microstructure and mechanical properties of three face centered cubic alloys processed by laser powder bed fusion. J Manuf Process 66:397–406. https://doi.org/10.1016/j.jmapro.2021.04.013
7. Pouille Q, Ladaci A, Lomello F, Cheymol G, Laffont G, Lerner A, Maskrot H, Girard S, Aubry P (2022) Impact on mechanical properties following a process interruption during additive manufacturing. Procedia CIRP 111:326–329. https://doi.org/10.1016/j.procir.2022.08.032
8. Richter J, Sajadifar SV, Niendorf T (2021) On the influence of process interruptions during additive manufacturing on the fatigue resistance of AlSi12. Additive Manuf 47:102346. https://doi.org/10.1016/j.addma.2021.102346
9. Stokes RM, Yadollahi A, Priddy MW, Bian L, Hammond VH, Doude HR (2022) Effects of build interruption and restart procedure on microstructure and mechanical properties of laser powder bed fusion Al-Si-10Mg. J Mater Eng Perform. https://doi.org/10.1007/s11665-022-07217-1
10. Mahtabi MB, Yadollahi A, Stokes RM, Young J, Doude HR, Priddy MW, Bian L (2022) Effects of process interruption during laser powder bed fusion on microstructural and mechanical properties of fabricated parts. In: Solid freeform fabrication 2022: Proceedings of the 33rd Annual international solid freeform fabrication symposium—an additive manufacturing conference. pp. 592–602. https://doi.org/10.26153/tsw/44128
11. Mahtabi M, Yadollahi A, Stokes R, Doude H, Priddy M (2023) Effect of build interruption during laser powder bed fusion process on structural integrity of Ti-6Al-4V. Eng Fail Anal 153:107626. https://doi.org/10.1016/j.engfailanal.2023.107626
12. VDI Verein Deutscher Ingenieure e.V. 2022-12-00, Additive Fertigungsverfahren—Pulverbettbasiertes Schmelzen von Metall mittels Laserstrahl (PBF-LB/M)—Fehlerkatalog—Fehlerbilder beim Laser-Strahlschmelzen, Vol. 25.030
13. DIN Deutsches Institut für Normung e.V. 2018-07-00, Metallische Werkstoffe—Härteprüfung nach Vickers—Teil1: Prüfverfahren, Vol. 77.040.10
14. VDI Verein Deutscher Ingenieure e.V. 2023-08-00, Additive Fertigungsverfahren—Strahlschmelzen metallischer Bauteile—Qualifizierung, Qualitätssicherung und Nachbearbeitung, 03.120.10, 25.020
15. DIN Deutsches Institut für Normung e.V. 2022-08-00, Prüfung metallischer Werkstoffe—Zugproben, Vol. 77.040.10
16. DIN Deutsches Institut für Normung e.V. 2020-06-00, Metallische Werkstoffe—Zugversuch - Teil 1: Prüfverfahren bei Raumtemperatur, Vol. 77.040.10
17. DIN Deutsches Institut für Normung e.V. 2018-12-00, Prüfung metallischer Werkstoffe—Umlaufbiegeversuch, Vol. 77.040.10
18. DIN Deutsches Institut für Normung e.V. 2022-12-00, Schwingfestigkeitsversuch—Durchführung und Auswertung von zyklischen Versuchen mit konstanter Lastamplitude für metallische Werkstoffproben und Bauteile, 19.060; 77.040.10

19. Goossens LR, Kinds Y, Kruth J-P, Van Hooreweder B (2018) On the influence of thermal lensing during selective laser melting. SFF Symp 2018:2267–2274

20. Andersen SA, Valente EH, Nadimpalli VK, Hansen HN, Pedersen DB (2019) A method for identification and quantification of thermal lensing in powder bed fusion. In: Proceedings of the 19th international conference and exhibition (EUSPEN 2019)

21. Mower TM, Long MJ (2016) Mechanical behavior of additive manufactured, powder-bed laser-fused materials. Mater Sci Eng: A 651:198–213. https://doi.org/10.1016/j.msea.2015.10.068

22. Beevers E, Brandão AD, Gumpinger J, Gschweitl M, Seyfert C, Hofbauer P, Rohr T, Ghidini T (2018) Fatigue properties and material characteristics of additively manufactured AlSi10Mg—effect of the contour parameter on the microstructure, density, residual stress, roughness and mechanical properties. Int J Fatigue 117:148–162. https://doi.org/10.1016/j.ijfatigue.2018.08.023

23. Du Plessis A, Beretta S (2020) Killer notches: The effect of as-built surface roughness on fatigue failure in AlSi10Mg produced by laser powder bed fusion. Additive Manuf 35:101424. https://doi.org/10.1016/j.addma.2020.101424

24. Lai W-J, Li Z, Ohja A, Li Y, Forsmark J, Engler C, Su X (2020) Effects of surface roughness and porosity on fatigue behavior of AlSi10Mg produced by laser powder bed fusion process. In: Structural integrity of additive manufactured materials and parts, pp. 229–246

25. Raja A, Cheethirala SR, Gupta P, Vasa NJ, Jayaganthan R (2022) A review on the fatigue behaviour of AlSi10Mg alloy fabricated using laser powder bed fusion technique. J Mater Res Technol 17:1013–1029. https://doi.org/10.1016/j.jmrt.2022.01.028